doi: 10.46793/EEE24-2.01P

Originalni naučni rad

UDK 621.354.2:621.352

Adaptive Models for Improved Battery Charging Systems

Danijel Pavković[*], Sandra Stanković[**], Karlo Kvaternik[***], Nikolina Sitar[****], Mihael Cipek*

[*] University of Zagreb, Faculty of Mechanical Engineering and Naval Architecture, Zagreb, Croatia
[**] Academy of Applied Technical and Preschool Studies Department of Niš, Niš, Serbia
[***] AVL-AST d.o.o., Zagreb, Croatia
[****] Rimac Technology, Sveta Nedelja, Croatia

Abstract – During its operation, sometimes it is a needed to swiftly replenish the battery from a partially depleted state, while strictly adhering to its technological limitations such as the battery terminal voltage and rated continuous charging current. To achieve this goal, this contribution outlines the dynamic battery recharging system, utilizing feedback provided by the nonlinear estimator of the battery state-of-charge (SoC) or SoC-related open-circuit-voltage (OCV). In the former case, the estimator is realized as an extended Kalman filter (EKF), while in the latter case it is implemented using the methodology of a System Reference Adaptive Model (SRAM), whose design is based on the Lyapunov stability theory. Thus-obtained innovative adaptive battery chargers are compared against the conventional constant-current/constant-voltage (CCCV) charging system, which relies solely on battery voltage feedback. A comprehensive comparative analysis is conducted through extensive simulations utilizing the nonlinear equivalent circuit model of the lithium titanate battery (LTO) cell.

Index Terms – Battery charging, State-of-charge, Nonlinear estimators, Extended Kalman filter (EKF), System Reference Adaptive Model (SRAM)

I INTRODUCTION

The widespread integration of renewable energy sources, such as solar and wind power, into the electricity grid presents exciting opportunities for a sustainable future [1]. However, their inherent variability necessitates robust energy storage solutions to bridge periods of low generation and ensures local grid stability [2]. Batteries play a crucial role in this context, enabling the storage and utilization of renewable energy when available, while providing reliable power when needed, as showcased for the cases of water desalinization systems [3] and sustainable eco-industrial enterprises [4].

Conventional battery charging systems, such as the widely used constant-current/constant-voltage (CCCV) method, prioritize simplicity and ease of implementation [5]. However, they lack the ability to adapt to individual battery characteristics or dynamic operating conditions [6]. This limitation can lead to suboptimal charging times, reduced battery life, and even safety concerns due to overcharging [7, 8].

Several techniques address battery voltage and temperature constraints. The MPC approach [9, 10] dynamically adjusts the charging current to honor the temperature bounds, while artificial intelligence approaches, such as fuzzy logic control [11] and neural networks [12], rely on data-driven learning to adapt to varying battery conditions. Offline approaches such as genetic algorithms [13, 14], dynamic programming [15], and multi-objective optimization [16] optimize the charging current profiles. However, the usefulness of the latter approach is limited by battery parameter variations during operation. To address this, online state-of- charge (SoC) estimation has been integrated with conventional charging control [17] to optimize the charging speed while respecting the charging current-related temperature limits. The additional benefit of SoC estimator-based approaches is in ensuring high precision of the final battery SoC at the end of the charging process.

Battery SoC estimation is typically based on the nonlinear battery model embedded within the nonlinear SoC estimator, typically realized in the form of an extended Kalman filter of EKF [18], wherein the battery equivalent circuit model used within the EKF-based estimator [19] can have different levels of complexity [20], or the battery can be represented by its equivalent electrochemical model [21]. Estimating the open-circuit-voltage (OCV) that is directly related to the SoC can be performed by utilizing Lyapunov stability theory and a System Reference Adaptive Model (SRAM) that dynamically estimates the battery model parameters in real time [22], and thus can be used for supervision of the charging process without requiring the explicit a-priori knowledge of the process model parameters [23]. A good overview of battery SoC estimation techniques can be found in [24].

Adaptive SoC feedback and OCV feedback systems for charging process speed-up have been previously proposed in [25] and [23], respectively. In these applications of the adaptive charging systems presented in [23] and [25], a $LiFePO_4$ battery cell characterized by the relatively moderate nominal rated charging rate of 0.3C (30% of charge capacity per hour) has been used [26]. The comprehensive simulation analysis presented in [23] and [25] has shown that by increasing the maximum charging current towards 0.7C in both the conventional charging benchmark and adaptive control strategies, adaptive control strategies can achieve about 25% speedup compared to the benchmark case of a conventional CCCV charging. The advent of next-generation lithium titanate or lithium titanium oxide (LTO) battery cells has motivated further research of these adaptive charging control strategies because these cells are characterized by superior performance in terms of maximum continuous charging current (with 1C charging rates having minimal effect on the battery cell aging), as well as superior thermal stability and overall robustness [27].

To this end, this paper presents and compares the previously

proposed adaptive charging systems from [23, 25], which were designed to overcome the limitations of conventional methods by means of augmenting (retrofitting) the conventional CCCV charging system with an additional feedback loop based on SoC-related information. Building upon established nonlinear estimation techniques, the presented approaches can achieve faster and safer charging while respecting battery safety constraints in terms of terminal voltage and continuous charging current limitations. The study presented in this paper assesses the benefits of charging strategies previously developed for earlier-generation and lower charging rate $LiFePO_4$ battery cell to the novel high charging rate LTO cell. It systematically examines in the MATLAB/Simulink simulation environment the effect of initial battery SoC and charging current limit to the relative speed-up of the two adaptive control strategies with respect to the conventional charging system benchmark, and the main results of this simulation study are confirmed by means of experiments.

The paper is organized as follows. Section II presents the charging system layout, whereas Section III presents the experimentally identified battery equivalent circuit model. Section IV outlines the three charging strategies whose performance (charging speed) is examined and compared in this paper, along with the SoC and OCV estimators used within the adaptive control strategies. Section V presents the results of comprehensive simulation assessment of adaptive control strategies with respect to the conventional charging benchmark, whereas Section VI presents the results of experimental verification of the proposed battery charging systems. Section VII presents a brief discussion of the obtained results, while the concluding remarks are given in Section VIII.

II Charging System Layout

Fig. 1 (right) depicts a conventional battery charging system schematic. The core topology is a buck DC/DC converter comprised of switching element Q (MOSFET), energy storage inductor L_c, and parallel freewheeling diode D. For active load scenarios (e.g., a battery cell), the optional series-connected blocking diode D_b safeguards against reverse current flow. Converter output voltage (u_c) is regulated by an embedded current controller. This controller receives its setpoint (i_{bR}) from a supervisory control layer, from either a battery voltage controller or a SoC management system [8], as discussed in subsequent sections.

Figure 1 (left) presents an equivalent circuit model for a battery cell. It features a series-connected ideal voltage source (U_{oc}) representing the cell's open-circuit voltage U_{oc} connected in series with a parallel RC circuit and an additional series resistance R_b. The above RC circuit models the cell's dominant electrolyte polarization behavior (with R_p being the polarization resistance, and C_p being the polarization capacitance). Finally, the cell's equivalent series resistance is represented by the resistor R_b.

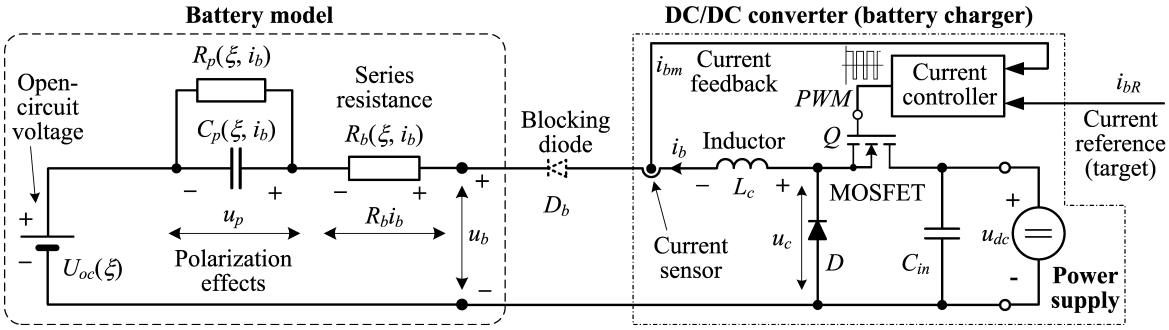

Figure 1. Battery charging system with buck converter and battery equivalent electrical circuit model [8]

III Battery Model

Applying the Kirchhoff's voltage law to the battery model in Fig. 1, the battery terminal voltage is expressed as follows [28]:

$$u_b = i_b R_b + u_p + U_{oc}. \tag{1}$$

Battery SoC (ξ) is defined as the time integral of battery current, normalized by battery charge capacity Q_b:

$$\xi = \frac{1_b}{Q}\int i_b dt \;\Leftrightarrow\; \dot{\xi} = \frac{i_{1b}}{Q} \tag{2}$$

while the polarization voltage u_p term in equation (2) can be expressed as [13]:

$$u_p = \frac{1}{\tau_p}\int (u_p - R_p i_b)dt \Leftrightarrow \dot{u}_p = \frac{u_p - R_p i_b}{\tau_p} \tag{3}$$

where $\tau_p = R_p C_p$ is the polarization time constant.

The designs of nonlinear estimators of battery SoC and OCV, which are presented subsequently, are based upon the battery terminal voltage equation (1) combined with the differential equation (2) and state-of-charge differential equation (3). In particular, equation (2) is used within the SRAM-based OCV estimator design, whereas both equations (2) and (3) are needed to define a suitable state-space model for the design of EKF-based state estimator.

Figures 2 and 3 depict experimentally derived relationships between the SoC, battery current, and battery model parameters of a commercial 30 Ah/2.4V/6C LTO cell's equivalent circuit model [28]. These include the OCV vs. SoC dependence, series resistance, polarization resistance, and polarization time constant $\tau_p = R_p C_p$. The presented data have been obtained under constant-temperature ambient conditions. The characteristics reveal marked SoC-dependence for all modeled parameters, particularly

at extreme SoC levels. These experimentally determined parameter maps (Figures 2 and 3) are directly integrated into Eqs. (1)-(3) within a MATLAB/Simulink simulation model. The model, having battery current (i_b) as input and battery terminal voltage (u_b) as output, is schematically represented by block diagram in Fig. 4.

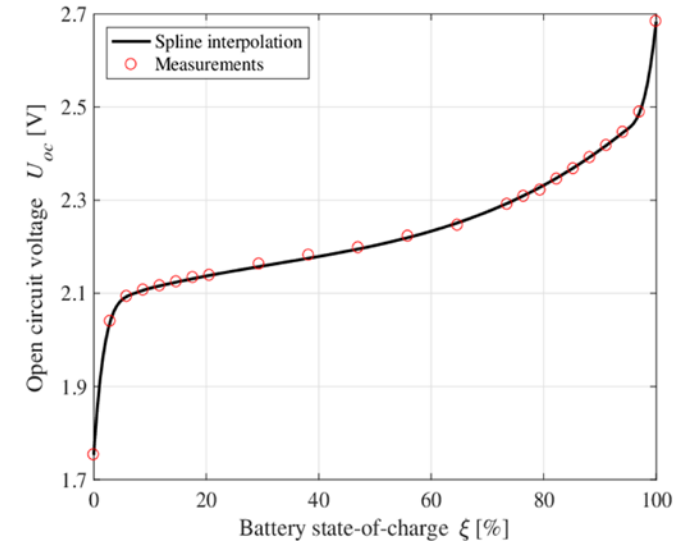

Figure 2. Battery OCV vs. SoC curve

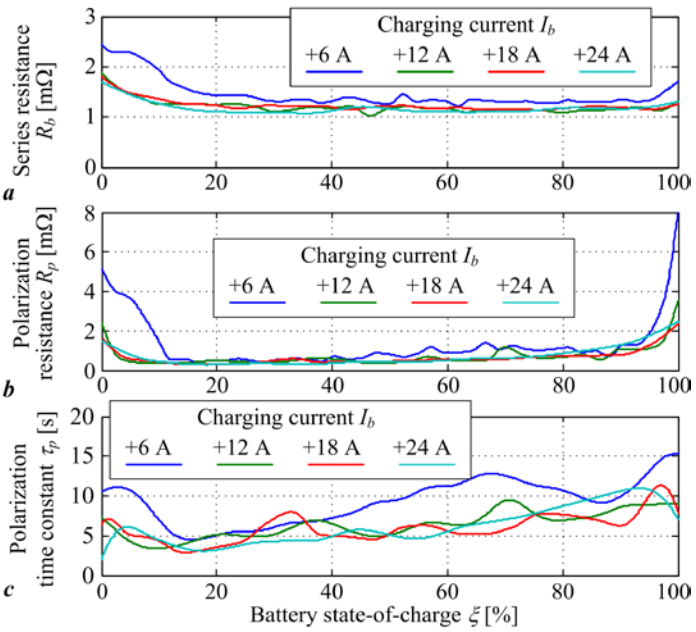

Figure 3. (a) Equivalent series resistance, (b) polarization resistance, and (c) polarization time constant curves

IV Control Systems under Investigation

Block diagrams in Fig. 5 depict the three battery charging control strategies from [5], [25] and [23]). Firstly, the conventional CCCV controller with voltage limiting (CCCV-VL), which is considered as a benchmark case is shown in Fig. 5a [5]. This charging control system uses a voltage limiting controller based on battery terminal voltage feedback (u_{bm}). The current reference (target value) i_{bR} combines the maximum charging current (I_{max}, used during the constant-current phase) and the controller's limiting command (i_{blim}), which reduces the charging current when u_{bm} exceeds its limit (target) value u_{blim}. The latter constant-voltage phase is characterized by asymptotically decreasing charging current and the battery terminal voltage approaching the SoC-dependent OCV $U_{oc}(\xi)$, i.e. $i_b \to 0$, $u_b \to U_{oc}$ [5].

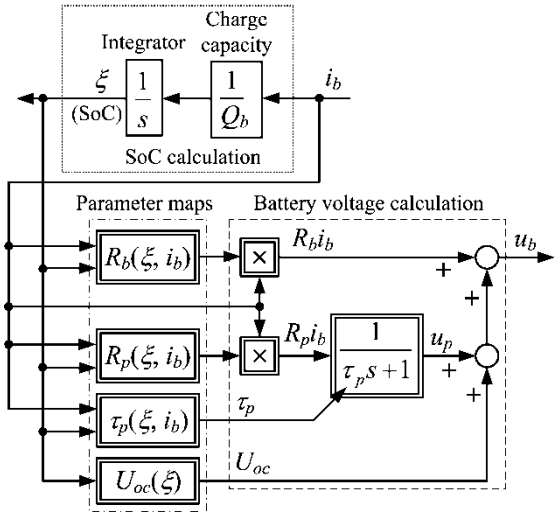

Figure 4. Block diagram of battery equivalent circuit model

Fig. 5b illustrates the so-called CCCV-SoC adaptive approach using SoC feedback [25]. Here, the principal SoC controller is provided with the SoC target value and produces the charging current reference i_{bR} (limited to I_{max} during the constant-current phase) based on SoC feedback provided by the SoC estimator. The SoC estimator, implemented in the form of an EKF, can be regarded as an adaptive digital twin (see e.g. [28]) of the battery cell, thus allowing for more targeted charging towards the fully charged state when compared to the conventional (CCCV-VL) charging system. The voltage limiting PI controller now provides a safety function by constraining the battery voltage to u_{blim}. Notably, this limit value (u_{blim}) can now be made higher than in the case of CCCV-VL strategy and is preset independently of the SoC control loop. Such modular control system structure allows conventional systems from Fig 5a to be easily upgraded with adaptive features.

Finally, Fig 5c shows an adaptive control system with the OCV controller, denoted herein as the CCCV-OCV control strategy [23]. The primary OCV controller uses the estimated OCV feedback, commanding the current reference i_{bR}, again limited to I_{max}. OCV feedback (U_{oc} estimate) is provided by the SRAM estimator. To estimate the battery model parameters in real-time, SRAM-based estimator requires continuous excitation via a pseudo-random binary sequence (PRBS) test signal Δi_{bR} superimposed to the overall current reference ($i_{bR} + i_{blim}$), see e.g. [23]. Similar to previous charging control strategies, the voltage limiting controller ensures safe operation by maintaining the battery terminal voltage below the limit value u_{blim} via its current command i_{blim}. Again, u_{blim} is preset independently of the target open-circuit voltage (OCV reference) U_{ocR} [23].

Figure 6 shows principal block diagram representations of the EKF-based SoC estimator from [25] and OCV estimator based

on SRAM principle from [23]. Both nonlinear estimators are implemented as feedback loop systems. In particular, these estimators attempt to minimize the model output prediction error e_m between the estimated battery voltage (battery model output) and the battery voltage measurement by means of corrective feedback action.

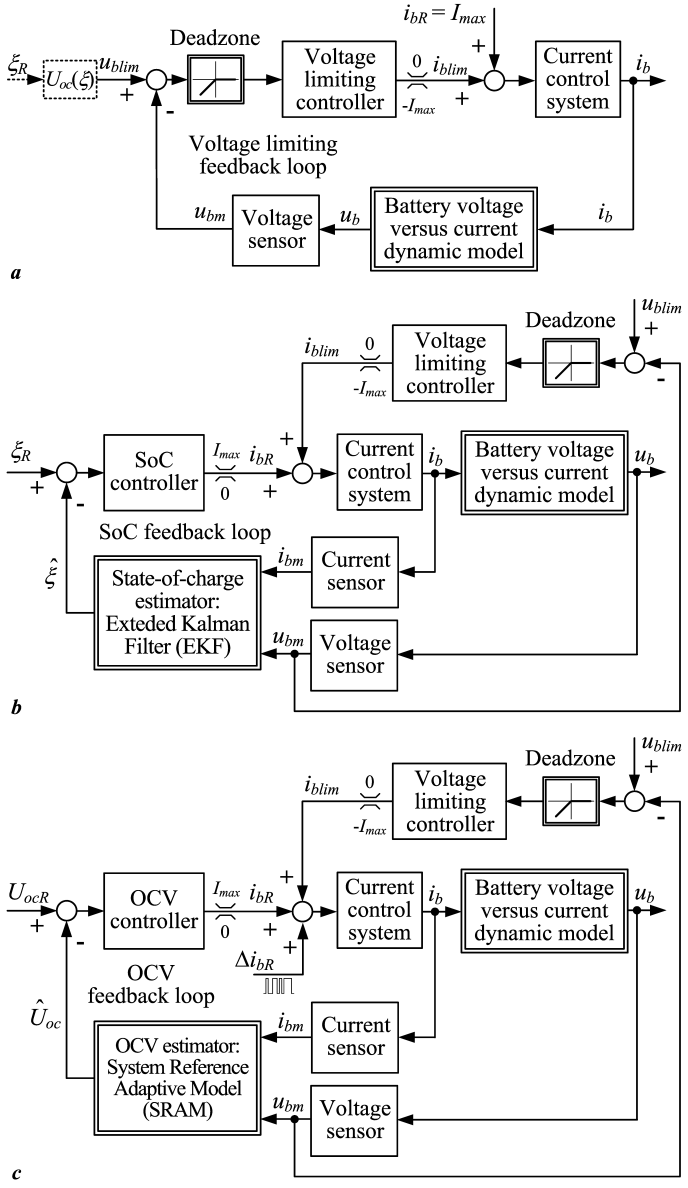

Figure 5. Block diagram of (a) CCCV-VL charging control strategy, (b) CCCV-SoC control strategy, and (c) CCCV-OCV control strategy

In the case of EKF-based SoC estimation (Fig. 6a), the estimated battery model output is obtained from the copy (digital twin) of the battery model (equations (1) – (3)) implemented with a-priori known parameter maps (Figs. 2 and 3), as illustrated in Fig. 4. The battery voltage prediction error is multiplied by Kalman filter gains matrix **K** and fed back to the model to compensate for the model following error e_m. The so-called optimal gains of the EKF-based estimator are calculated based on the linearized process model (Fig. 6a). The SRAM-based battery model parameters estimator (Fig. 6b) uses the known structure of the battery model and adapts the model parameters on-line by using the Lyapunov stability criterion-based adaptation law [23] which requires battery voltage and current filtering and related extraction of battery current time derivative. These signals are then combined with the adaptive model prediction error e_m to provide the adaptation law for on-line parameter updates. As mentioned above, the SRAM-based parameter estimator requires that the CCCV-OCV control system is subjected to persistent excitation realized by means of the superimposed PRBS signal Δi_{bR} (see Fig. 5c).

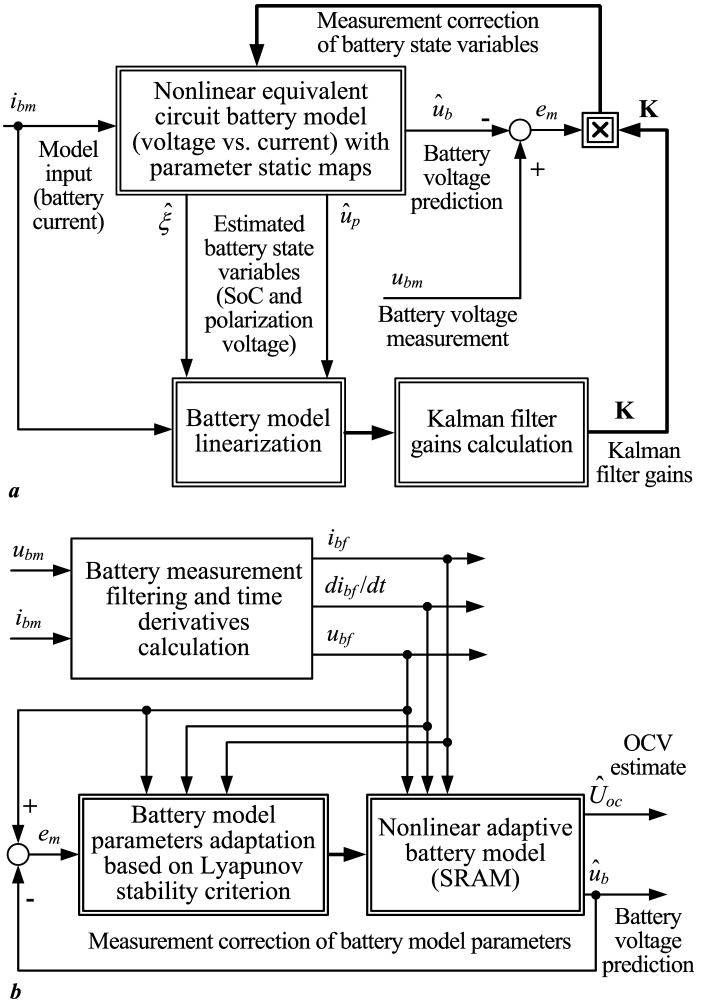

Figure 6. Principal block diagrams of (a) EKF-based battery state-of-charge estimator and (b) battery OCV estimator based on SRAM principle

Detailed design procedures for CCCV-VL, CCCV-SoC and CCCV-OCV control systems and the respective battery state and parameter estimators can be found in references [25] and [23].

V Comparative Simulation Results

Simulations comparing various charging strategies considered different initial battery SoC levels (ξ_0) and constant-current stage charging current limits (I_{max}). Table 1 summarizes these values and additional key simulation parameters. Notably, the charging process terminates in the constant-voltage stage when the battery current falls below the turn-off current (I_{min}).

Table 1. Simulation model and charging scenarios parameters.

Parameter	Value
Battery cell charge capacity Q_b	30 Ah
Charging current rated value (1C rate)	30 A
Charging strategy current maximum values I_{max} in simulation scenarios	30 A, 24 A, 18 A, 12 A (1C, 0.8C, 0.6C, 0.4C)
Charging strategy turn-off current I_{min}	0.3 A (0.01C)
Battery SoC initial conditions ξ_0	20%, 40%, 60%, 80%
CCCV-VL voltage limit u_{blim}	2.68 V
CCCV-SoC/OCV voltage limit u_{blim}	2.72 V
Battery SoC target value ξ_R	100%

Figure 7 shows the comparative simulation responses of the presented charging strategies with I_{max} = 30A, which corresponds to 1C rate for the LTO cell under examination [30], and initial SoC at 20%. Both the CCCV-SoC and CCCV-OCV strategies exhibit a sharper transition to zero current post constant-current charging compared to the CCCV-VL strategy's asymptotic transient towards zero current. This results in shorter charging times (see top plots in Figs. 7a and 7b), facilitated by the CCCV-SoC and CCCV-OCV strategy's ability to briefly exceed terminal voltage limits during the final phase (see battery voltage traces in Figs. 7a and 7b). Both adaptive control strategies (CCCV-SoC and CCCV-OCV) achieve near-identical final SoC values. The EKF-based SoC estimator accurately tracks the battery's actual SoC (Fig. 7a), whereas the SRAM estimator OCV tracking ability is somewhat less favorable in the initial portion of the response (Fig. 7b). The latter can be partly attributed to the rate of change of OCV when SoC is quite low, as shown in Fig. 2.

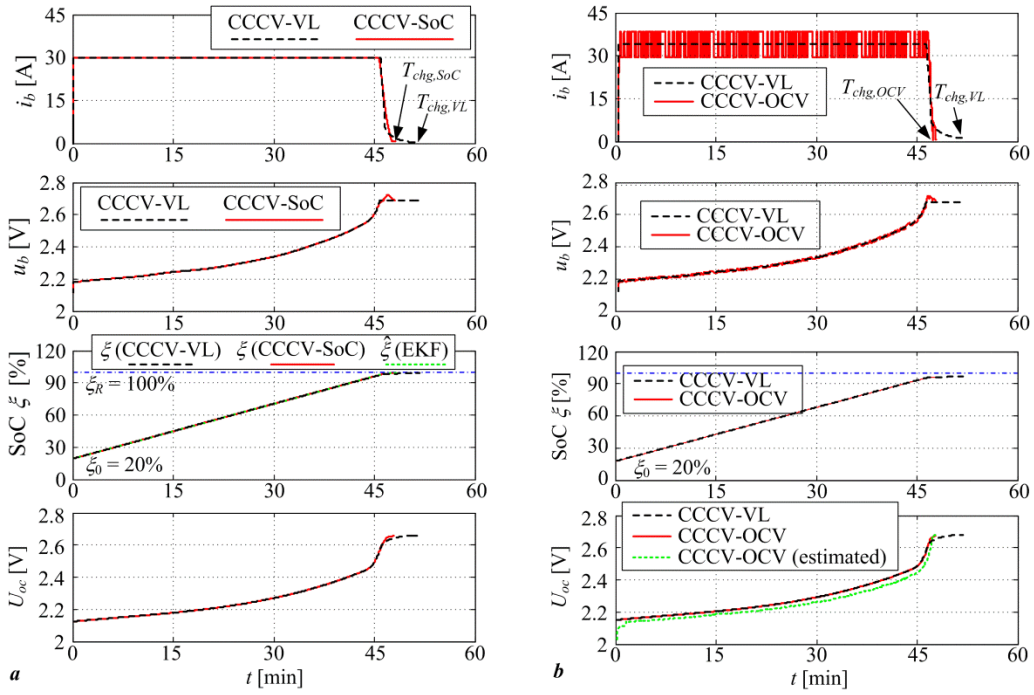

Figure 7. Comparative simulation results: (a) CCCV-VL vs. CCCV-SoC strategy and (b)CCCV-VL vs. CCCV-OCV strategy for 30 A current limit and initial SoC of 20%

Figure 8 presents the relative charging speedup factors κ_{chg} and the final SoC mismatch $\Delta\xi_{fin}$ values for simulation scenarios given in Table I for both adaptive charging strategies (CCCV-SoC and CCCV-OCV) compared to conventional CCCV-VL charging strategy. The relative speedup factor κ_{chg} of the adaptive CCCV-SoC and CCCV-OCV charging strategies to the conventional CCCV-VL strategy is calculated as the ratio of the difference in charging times as follows:

$$\kappa_{chg} = \left(1 - \frac{T_{chg,SoC(OCV)}}{T_{chg,VL}}\right) \cdot 100\% \quad (4)$$

where $T_{chg,VL}$, $T_{chg,SoC}$ and $T_{chg,OCV}$ are CCCV-VL, CCCV-SoC and CCCV-OCV strategy charging times, respectively.

The second criterion that can be used to assess the presented charging strategies is final SoC mismatch $\Delta\xi_{fin}$ between the CCCV-VL and the CCCV-SoC strategy, given by:

$$\Delta\xi_{fin} = \xi_{fin,VL} - \xi_{fin,SoC(OCV)} \quad (5)$$

where $\xi_{fin,VL}$, $\xi_{fin,SoC}$ and $\xi_{fin,OCV}$ are the final SoC values obtained by the CCCV-VL, CCCV-SoC and CCCV-OCV strategies.

The results presented in Fig. 8 clearly demonstrate consistent charging time reduction of adaptive charging control strategies compared to the CCCV-VL benchmark. Recharging speedup is most prominent (over 20%) at higher charging currents (higher I_{max}) and initial SoC (higher ξ_0). As explained in Figs. 7 and 8, CCCV-SoC and CCCV-OCV exhibit a slightly lower final SoC (ξ_{fin}) due to their sharper current termination. However, the final SoC mismatch $\Delta\xi_{fin}$ remains consistently below 0.2%, thus being inconsequential in practical applications.

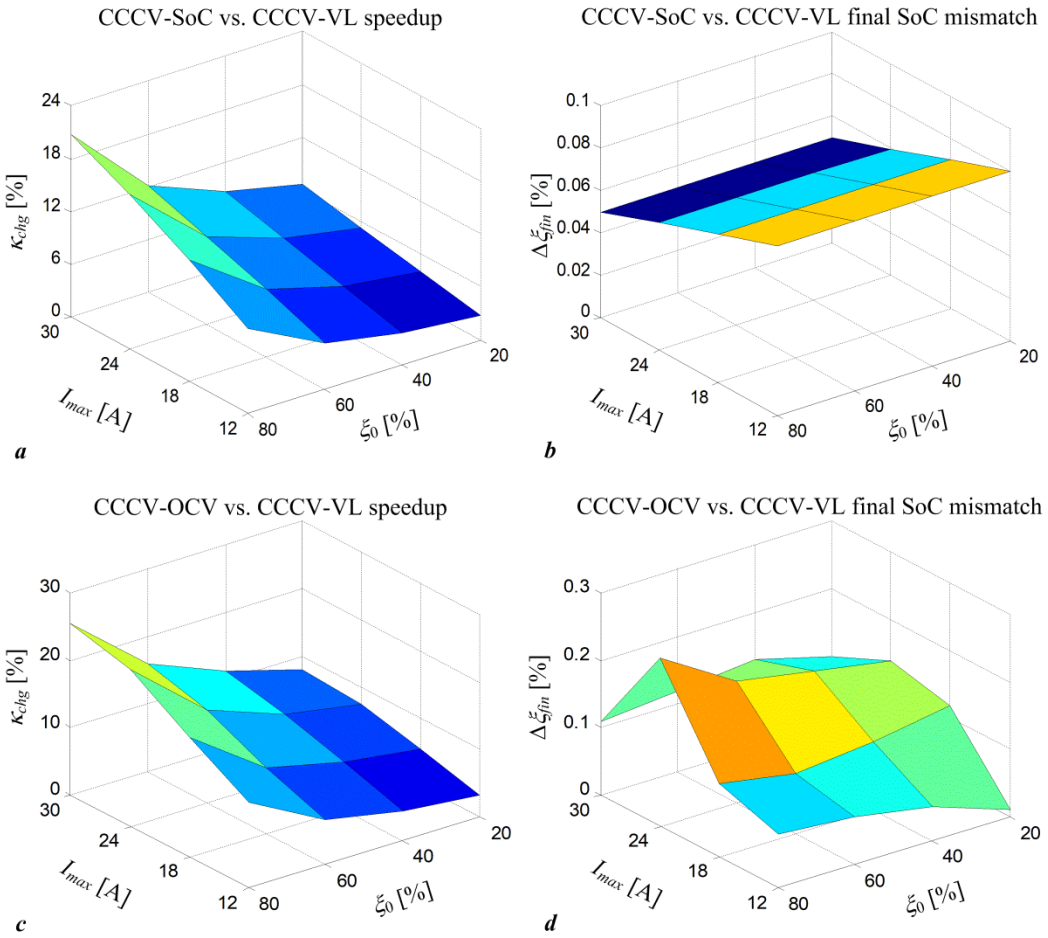

Figure 8. Comparative performance indices CCCV-SoC and CCCV-OCV strategies compared to CCCV-VL benchmark: (a) CCCV-SoC charging speedup and (b) final SoC mismatch, and (c) CCCV-OCV charging speedup and (d) final SoC mismatch

VI Experimental Results

Experimental verification of the proposed charging concept has been carried out on the battery test setup shown in Fig. 9.

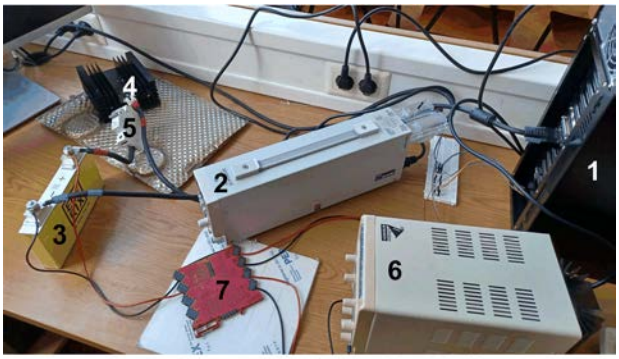

Legend: 1 – control computer equipped with acquisition and control cards; 2 – DC/DC power converter; 3 – lithium-titanate battery cell (30 Ah / 2.4 V); 4 – blocking diode; 5 – circuit breaker; 6 – auxiliary 24 V_{dc} power supply; 7 – battery terminal voltage isolation amplifier

Figure 9. Photograph of the battery experimental setup

An industrial control computer "1" equipped with cards for acquisition and control executes the dedicated real-time control code and commands appropriate current reference to the laboratory power source "2" for charging the commercial 30Ah/2.4V/6C LTO battery cell "3" [30]. A high-power blocking diode "4" prevents accidental reverse current flow and protects the circuit in the case of incorrect connection of power terminals, while a circuit breaker "5" is used for over-current protection. For galvanic isolation of the battery voltage measurement analog input from the DC/DC converter power terminals, the setup also features an isolation amplifier for voltage measurement "7" with its own separate power supply "6".

Figures 10 and 11 show the comparative experimental results of the proposed control strategies. Tests were conducted with an upper charging current limit of 18A (0.6C) and two initial SoC values: ξ_0 = 4.2% (very depleted) and ξ_0 = 69.5% (medium-high). The initial SoC values were determined from the battery's idling voltage (u_0) measured before the charging started (see Figs. 10 and 11). The study did not consider higher charging current limits (0.8C and 1C) due to a safety constraint: increased heat losses at the reverse-flow blocking diode. Results in Figs. 10 and 11 confirm that all three charging strategies can successfully bring the battery SoC (OCV) towards the target value which corresponds to 100% battery SoC. Moreover, the experimental results also confirm the key findings of the simulation analysis conducted for a broader range of initial SoC conditions and

current limit values. Specifically, they confirm that the CCCV-OCV and CCCV-OCV control strategies can achieve a noticeable speedup in the charging process with respect to the conventional CCCV-VL charging strategy.

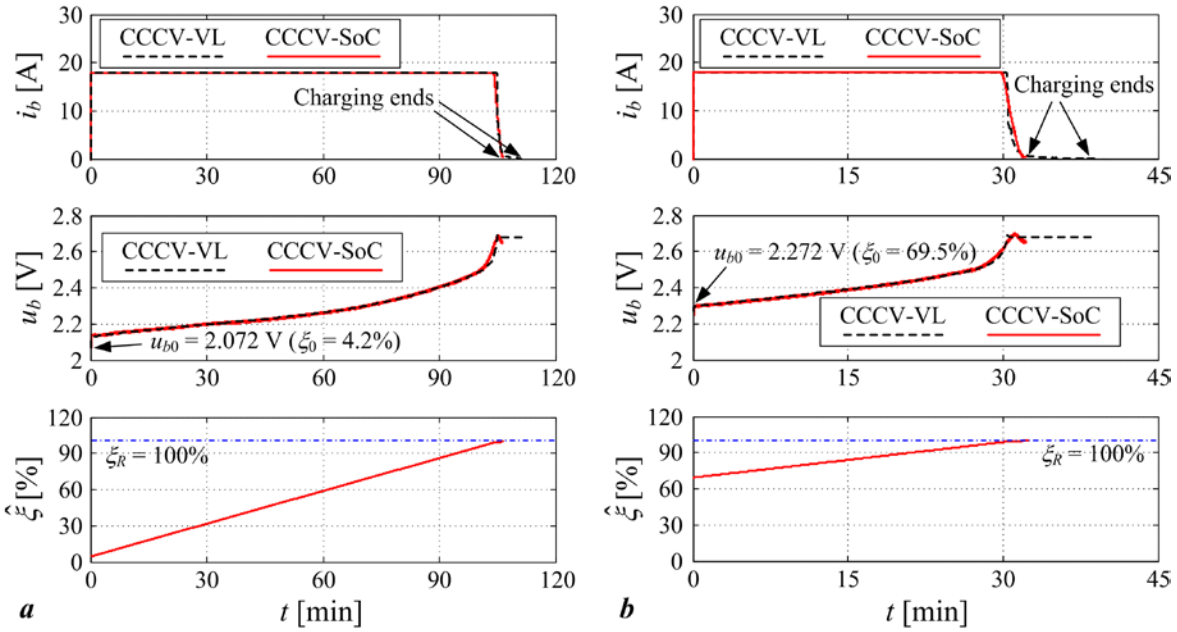

Figure 10. Comparative experimental results of CCCV-VL and CCCV-SoC strategies for 18 A current limit and initial SoC of (a) 4.2% and (b) 69.5%

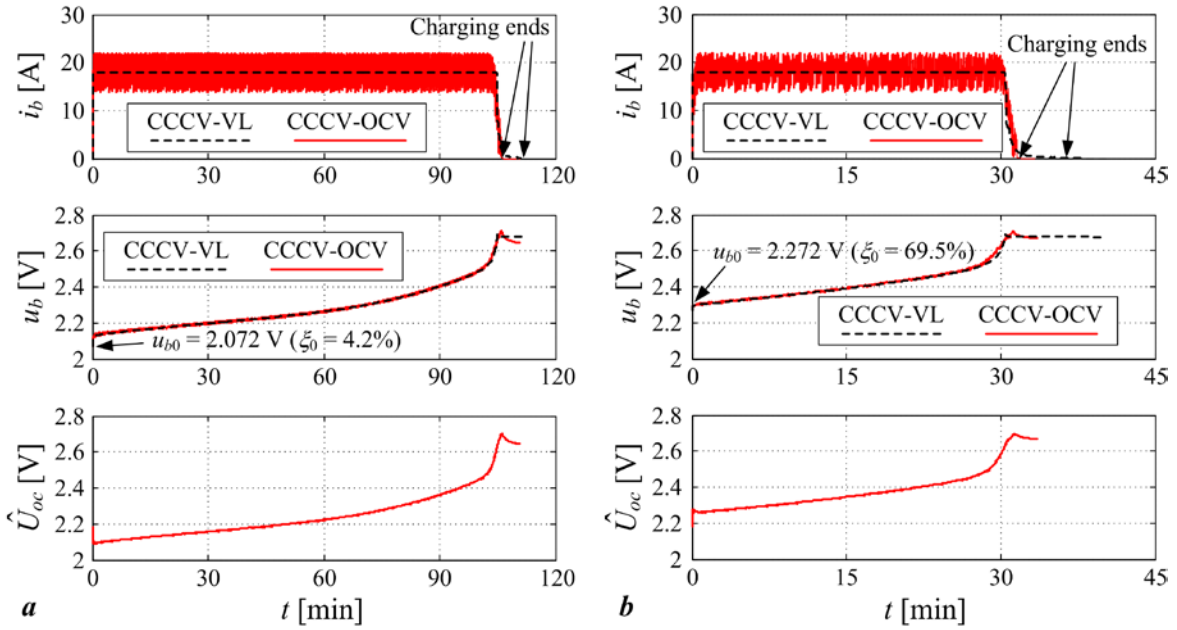

Figure 11. Comparative experimental results of CCCV-VL and CCCV-OCV strategies for 18 A current limit and initial SoC of (a) 4.2% and (b) 69.5%

VII Discussion of Results

The presented research addresses the inherent limitations of conventional CCCV battery charging systems. By employing more sophisticated model-based adaptive control strategies, such as the proposed EKF-based CCCV-SoC and SRAM-based CCCV-OCV strategy, significant improvements in charging performance can be demonstrated. The core strengths of these adaptive systems lie in their ability to estimate key battery parameters (SoC or OCV) in real-time using nonlinear estimators. This continuous monitoring enables optimized charging strategies that adapt to the specific battery's characteristics and operating conditions.

Simulation results convincingly illustrate the advantages of the adaptive charging strategies. Both methods exhibit notably faster charging times compared to the conventional CCCV-VL benchmark, particularly at higher charging currents and initial

SoC levels. This speedup highlights the ability of adaptive systems to push operational boundaries while still within safe operating limits. Moreover, both the EKF and SRAM-based charging methods demonstrate remarkable consistency in achieving the desired final SoC, with negligible discrepancies compared to conventional charging. In addition, all three charging strategies have been experimentally verified, and experimental results support the findings of the comprehensive simulation study in terms of charging speed-up when adaptive charging strategies are used. This indicates that adaptive charging strategies could be used in future practical applications.

Despite the clear benefits demonstrated, it is important to acknowledge the potential challenges associated with model-based adaptive charging approaches. Accuracy is dependent on the quality of the underlying battery model, parameter identification, and sensor measurements. Further research could focus on enhancing the robustness of these systems to parameter variations and exploring the inclusion of temperature compensation mechanisms. Additionally, while simulations offer valuable initial insights, experimental validation under real-world conditions will be essential for full technological maturation.

VIII Conclusion

The presented work demonstrates the effectiveness of adaptive charging systems in overcoming the limitations of traditional CCCV battery charging approaches. The developed EKF-based CCCV-SoC and SRAM-based CCCV-OCV systems offer a significant improvement in battery charging speed, wherein comprehensive simulations showcase the consistent reduction in charging time while maintaining the desired final SoC levels.

The potential applications of these adaptive methods extend far beyond the initial simulation study. Their ability to optimize charging performance in terms of charging speed while not perceptibly affecting the battery lifespan makes them highly attractive for integration into renewable energy systems, electric vehicles, and other battery-dependent applications. Future work can thus be focused on more extensive field tests and exploration of complementary control techniques that can further unlock the potential of the adaptive model-based charging control systems, with many practical implications such as more efficient and sustainable battery energy storage solutions.

Acknowledgement

Research supported by the European Commission through the Horizon 2020 project “Maximizing the impact of innovative energy approaches in the EU islands” (INSULAE).

References

[1] Zakariazadeh, A., Ahshan, R., Al Abri, R., Al-Abri, M. Renewable energy integration in sustainable water systems: A review. Cleaner Engineering and Technology, Vol. 18, No. 100722, 2024. https://doi.org/10.1016/j.clet.2024.100722

[2] Hassan, Q., Algburi, S., Sameen, Z.A., Salman, H.M., Jaszczur, M. A review of hybrid renewable energy systems: Solar and wind-powered solutions: Challenges, opportunities, and policy implications, Results in Engineering, Vol. 20, No. 101621, 2023. https://doi.org/10.1016/j.rineng.2023.101621

[3] Shokri, A., Fard, M.S. A sustainable approach in water desalination with the integration of renewable energy sources: Environmental engineering challenges and perspectives, Environmental Advances, Vol. 9, No. 100281, 2022. https://doi.org/10.1016/j.envadv.2022.100281

[4] Neri, A., Butturi, M.A. Lolli, F., Gamberini, R. Inter-firm exchanges, distributed renewable energy generation, and battery energy storage system integration via microgrids for energy symbiosis, Journal of Cleaner Production, Vol. 414, No. 137529, 2023. https://doi.org/10.1016/j.jclepro.2023.137529

[5] Pavković, D., Lobrović, M., Hrgetić, M., Komljenović, A., Smetko, V. Battery current and voltage control system design with charging application, In Proc. *IEEE Conference on Control Applications (CCA 2014)*, Juan Les Antibes, France, pp. 1133-1138, 11 December 2014. https://doi.org/10.1109/CCA.2014.6981481

[6] Kandasamy, V., Venkatesan, M. Adaptive electric vehicle charging method to improve the battery life, In Proc. *2nd International Conference on Advancements in Electrical, Electronics, Communication, Computing and Automation (ICAECA)*, Coimbatore, India, pp. 1-4, 16-17 June 2023. https://doi.org/10.1109/ICAECA56562.2023.10200210

[7] Dubarry, M., Qin, N., Brooker, P. Calendar aging of commercial Li-ion cells of different chemistries – A review, Current Opinion in Electrochemistry, Vol. 9, pp. 106-113, 2018. https://doi.org/10.1016/j.coelec.2018.05.023

[8] Chen, Y., Kang, Y., Zhao, Y., Wang, L., Liu, J., Li, Y., Liang, Z., He, X., Li, X., Tavajohi, N., Li, B. A review of lithium-ion battery safety concerns: The issues, strategies, and testing standards, Journal of Energy Chemistry, Vol. 59, pp. 83-99, 2021. https://doi.org/10.1016/j.jechem.2020.10.017

[9] Pozzi, A., Raimondo, D.M. Stochastic model predictive control for optimal charging of electric vehicles battery packs, Journal of Energy Storage, Vol. 55, Part A, No. 105332, 2022. https://doi.org/10.1016/j.est.2022.105332

[10] Xie, S., Hu, X., Qi, S., Tang, X., Lang, K., Xin, Z., Brighton, J. Model predictive energy management for plug-in hybrid electric vehicles considering optimal battery depth of discharge, Energy, Vol. 173, pp. 667-678, 2019. https://doi.org/10.1016/j.energy.2019.02.074

[11] Hsieh, G.C., Chen, L.R., Huang, K.S. Fuzzy-controlled li-ion battery charge system with active state-of-charge controller, IEEE Transactions on Industrial Electronics, Vol. 48, No. 3, pp. 585-593, 2001. https://doi.org/10.1109/41.925585

[12] Fan, Y., Wu, J., Chen, Z., Wu, H., Huang, J., Liu, B. Data-driven state-of-charge estimation of lithium-ion batteries. In Proc. *8th International Conference on Power Electronics Systems and Applications (PESA 2020)*, Hong Kong, China, pp. 1-5, 07-10 December 2020. https://doi.org/10.1109/PESA50370.2020.9344017

[13] Jiang, L., Huang, Y., Li, Y., Yu, J., Qiao, X., Huang, C., Cao, Y. Optimization of variable-current charging strategy based on SOC segmentation for Li-ion battery, IEEE Transactions on Intelligent Transportation Systems, Vol. 22, No. 1, pp. 622-629, 2021. https://doi.org/10.1109/TITS.2020.3006092

[14] Vo, T.T., Chen, X., Shen, W., Kapoor, A. New charging strategy for lithium-ion batteries based on the integration of Taguchi method and state of charge estimation, Journal of Power Sources, Vol. 273, pp. 413-422, 2015. https://doi.org/10.1016/j.jpowsour.2014.09.108

[15] Chen, Z., Xia, B., Mi, C. C., Xiong, R. Loss-minimization-based charging strategy for Lithium-Ion battery, IEEE Transactions on Industry Applications, Vol. 51, No. 5, pp. 4121-4129, 2015. https://doi.org/10.1109/TIA.2015.2417118

[16] Liu, K., Li, K., Ma, H., Zhang, J., Peng, Q. Multi-objective optimization of charging patterns for lithium-ion battery management, Energy Conversion and Management, Vol. 159, pp. 151-162, 2018. https://doi.org/10.1016/j.enconman.2017.12.092

[17] Lee, K.T., Dai, M.J., Chuang, C.C. Temperature-compensated model for Lithium-Ion polymer batteries with extended Kalman Filters State-of-charge estimation for an implantable charger, IEEE Transactions on Industrial Electronics, Vol. 65, No. 1, pp. 589-596, 2018.https://doi.org/10.1109/TIE.2017.2721880

[18] Xiong, R., He, H., Sun, F., Zhao, K. Evaluation on state of charge estimation of batteries with adaptive extended Kalman filter by experiment approach, IEEE Transactions on Vehicular Technology, Vol. 62, No. 1, pp. 108-117. 2013. https://doi.org/10.1109/TVT.2012.2222684

[19] He, H., Xiong, R., Zhang, X., Sun, F., Fan, J. State-of-Charge Estimation of the Lithium-Ion Battery Using an Adaptive Extended Kalman Filter Based on an Improved Thevenin Model, IEEE Transactions on Vehicular Technology, Vol. 60, No. 4, pp. 1461-1469, 2011.

https://doi.org/10.1109/TVT.2011.2132812

[20] Sepasi, S., Ghorbani, R., Liaw, B. Y. Improved extended Kalman filter for state of charge estimation of battery pack, Journal of Power Sources, Vol. 255, pp. 368-376, 2014. https://doi.org/10.1016/j.jpowsour.2013.12.093

[21] Di Domenico, D., Stefanopoulou, A., Fiengo, G. Lithium-Ion Battery State of Charge and Critical Surface Charge Estimation Using an Electrochemical Model-Based Extended Kalman Filter, ASME Journal of Dynamic Systems, Measurement, and Control, Vol. 132, No. 6, 061302-1, 2010. https://doi.org/10.1115/1.4002475

[22] Othman, B.M., Salam, Z., Husain, A. R. A computationally efficient adaptive online state-of-charge observer for Lithium-ion battery for electric vehicle, Journal of Energy Storage, Vol. 49, No. 104141, 2022. https://doi.org/10.1016/j.est.2022.104141

[23] Pavković, D., Kasać, J., Krznar, M., Cipek, M. Adaptive constant-current/constant-voltage charging of a battery cell based on cell open-circuit voltage estimation, World Electric Vehicle Journal, Vol. 14, No. 6, pp. 155, 2023. https://doi.org/10.3390/wevj14060155

[24] He, J., Meng, S., Yan, F. A comparative study of SOC estimation based on equivalent circuit models, Frontiers in Energy Research, Vol. 10, No. 914291, 2022. https://doi.org/10.3389/fenrg.2022.914291

[25] Pavković, D., Premec, A., Krznar, M., Cipek, M. Current and voltage control system designs with EKF-based state-of-charge estimator for the purpose of $LiFePO_4$ battery cell charging, Optimization and Engineering, Vol. 23, pp. 2335-2363, 2022. https://doi.org/10.1007/s11081-022-09728-1

[26] GWL/Power Group, SE100AHA cell specification. http://www.ev-power.eu/CALB-40Ah-400Ah/SE100AHA-Lithium-Cell-LiFePO4-3-2V-100Ah.html [pristupljeno 20.02.2024]

[27] Nemeth, T., Schröer, P., Kuipers, M., and Sauer, D. U. Lithium titanate oxide battery cells for high-power automotive applications - Electro-thermal properties, aging behavior and cost considerations, Journal of Energy Storage, Vol. 31, No. 101656, 2020. https://doi.org/10.1016/j.est.2020.101656

[28] Kvaternik, K., Pavković, D., Kozhushko, Y., Cipek, M., Krznar, M. Lithium-Titanate Battery Cell Experimental Identification and State-of-Charge Estimator Design, In Proc. *18th Conference on Sustainable Development of Energy, Water and Environment Systems (SDEWES 2023)*, Dubrovnik, Croatia, No. 36, 24-29 September 2023.

[29] VanDerHorn, E., Mahadevan, S. Digital Twin: Generalization, characterization and implementation, Decision Support Systems, Vol. 145, No. 113524, 2021. https://doi.org/10.1016/j.dss.2021.113524

[30] ELERIX EX-30TK Extreme Power LTO Cell, VDA size 173/100, Technical Specification, https://faktor.de/out/media/ELERIX-EX-T30K-QuickDatasheet.pdf [pristupljeno 20.02.2024]

AUTHORS

Danijel Pavković – Prof. dr. sc., University of Zagreb, Faculty of Mechanical Engineering and Naval Architecture, Zagreb, Croatia, danijel.pavkovic@fsb.unizg.hr, ORCID 0000-0001-8045-5109
Sandra Stanković – MS env. eng., Academy of Applied Technical and Preschool Studies Department of Niš, Niš, Serbia, sandra.stankovic@akademijanis.edu.rs, ORCID 0000-0002-0466-1426
Karlo Kvaternik – mag. ing. mech., AVL-AST d.o.o., Zagreb, Croatia, karlo.kvaternik@avl.com
Nikolina Sitar – mag. ing. mech., Rimac Technology, Sveta Nedelja, Croatia, nikolina.sitar@rimac-technology.com
Mihael Cipek – Doc. dr. sc., University of Zagreb, Faculty of Mechanical Engineering and Naval Architecture, Zagreb, Croatia, mihael.cipek@fsb.unizg.hr, ORCID 0000-0002-0611-8144

Adaptivni modeli za poboljšane sisteme punjenja baterija

Rezime **-** U procesu operativnog delovanja, periodično se javlja potreba za brzim dopunjavanjem baterije iz delimično ispražnjenog stanja, uz striktno poštovanje njenih tehnoloških ograničenja kao što su napon baterije i nominalna kontinuirana struja punjenja. Da bi se postigao ovaj cilj, ovaj rad opisuje sistem dinamičkog punjenja baterije, koristeći povratnu informaciju koju daje procenjivač (estimator) stanja napunjenosti baterije (SoC) ili napona otvorenog kola (OCV) koji je usko povezan sa SoC-om. U prvom slučaju, estimator je realizovan kao prošireni Kalmanov filter (EKF), dok je u drugom slučaju implementiran primenom metodologije Sistemskog referentnog adaptivnog modela (SRAM), čiji je dizajn zasnovan na teoriji stabilnosti Ljapunova. Tako dobijeni inovativni adaptivni punjači baterija upoređuju se sa konvencionalnim sistemom punjenja konstantnom strujom/konstantnim naponom (CCCV), a koji se oslanja isključivo na povratnu vezu po naponu baterije. Sveobuhvatna komparativna analiza je sprovedena kroz opsežne simulacije koristeći model nelinearnog ekvivalentnog kola ćelije litijum-titanat (LTO) baterije.

Klučne reči **-** Punjenje baterije; stanje napunjenosti; nelinearni procenjivači; prošireni Kalmanov filter (EKF); sistemski referentni adaptivni model (SRAM)